Electrosynthesis of Cu−Se Films on Copper Electrodes in Alkaline Media: A Voltammetric, Electrochemical Quartz Crystal Microbalance and *I*/*t* Transient Study

Ricardo Córdova,* Cristina López, Marco Orellana, Paula Grez, Ricardo Schrebler, and Rodrigo del Río

Instituto de Química, Pontificia Universidad Católica de Valparaíso, Casilla 4059, Valparaíso, Chile

Received: June 10, 2004; In Final Form: December 15, 2004

The electroformation of Cu−Se phases, obtained by selenizing a thin film of copper deposited on the quartz/gold electrode system, was studied with an electrochemical quartz crystal microbalance (EQCM) and by cyclic voltammetry (CV) in an alkaline solution (0.05 M $Na_2B_4O_7$) containing selenide ion. Potentiodynamic parameters showed that the formation of the initial Cu−Se phases ($Cu_{2-x}Se/Cu_3Se_2$) is ruled by an irreversible diffusion controlled mechanism, where a first electron transfer is the rate-determining step. A CV study was also performed with a bulk copper electrode in 1 M NaOH solution containing selenide ion. The deconvolution of the anodic and cathodic *I*/*E* profiles corresponding to the electroformation and electroreduction of the Cu−Se film formed allowed us to establish that, depending on the anodic potential limit of the potentiodynamic scan, the Cu−Se phases formed were either a mixture of $Cu_{2-x}Se/Cu_3Se_2$ or $Cu_{2-x}Se/Cu_3Se_2/CuSe$. An EQCM study showed that, during the initial stage of Cu−Se phase electroformation, water molecules were released from the electrode. In advanced stages of the process, when the electrode was completely covered by Cu−Se compounds, selenide anions were adsorbed on the formed phase. When the anodic potential limit was extended to −0.2 V, copper oxide compounds were formed. The analysis of the cathodic charge related to Cu−Se phase electroreduction and Energy Dispersive X-ray Spectroscopy (EDXS) analysis confirmed that when the anodic limit was −0.8 V, a mixture of different Cu−Se phases was formed. A *I*/*t* transient study performed with a bulk copper electrode in alkaline solution containing selenide established that the nucleation and growth mechanism (NGM) of the Cu−Se phases takes place through an initial bidimensional-instantaneous nucleation (IN2D), followed by four bidimensional-progressive nucleations (PN2D). These results and atomic force microscopy (AFM) experiences supported that the growth of the Cu−Se films occurs through a layer-by-layer mechanism.

1. Introduction

Metal chalcogenide compounds have a semiconductor nature, and they are of considerable technical interest in the field of electronics and electrooptical devices. Intensive research has been performed in the past to study the production and characterization of these compounds under the form of thin films. The electrodeposition of multinary compounds of practical use offers a reduced cost in comparison with the chemical bath deposition method and the chemical vapor deposition method. This is the case, for instance, of copper indium diselenide compound ($CuInSe_2$, CIS) which has received considerable attention in recent years in photovoltaic devices. CIS thin films are grown by co-deposition of Cu, In, and Se simultaneously.[1−5] Both CIS and its homologue Cu (In,Ga)Se_2 (CIGS) are highly promising absorber materials to obtain low cost polycrystalline thin film solar cells. CIS has an almost ideal band gap of ∼1 eV and a high absorption coefficient at photon energies above the band gap. The study of the copper/selenide system has been considered in the intermediate stages of CIS electrosynthesis as well as in the application of Cu_2Se as a window layer for solar cells.[6−7]

Pejova et al.[8] studied the deposition of different phases of Cu−Se compounds using a chemical method. This method was based on the decomposition of selenosulfate in an alkaline medium containing a Cu(II) salt and a suitable complexing agent. The different phases obtained (Cu_2Se and Cu_3Se_2) were characterized by X-ray diffraction (XRD) and other optical measurements.

Marlot et al.[9] used a rotating electrochemical quartz crystal microbalance (REQCM) to study the electrodeposition of Cu−Se compounds from aqueous solutions of $CuSO_4$ and H_2SeO_3. The composition of the films obtained was determined in situ by means of the simultaneous measurements of the quantity of charge and mass gains. Besides, the compositions of the films deposited were dependent on hydrodynamic conditions of the solution and the electrolyte composition used.

The electroformations of Cu−Se phases by the deposition of copper onto selenium covered gold electrodes were studied by different electrochemical techniques.[10] Through the analysis of the *I*/*t* transients, the potential edge where the initial stages of Cu−Se compounds start was established.[3] A general reaction scheme that considers the formation of CuSe and $Cu_{2-x}Se$ compounds was proposed by taking into account the charges involved in the anodic redissolution of the Cu−Se deposits previously electrosynthesized.

Kemell et al.[11] studied the one-step electrodeposition of $Cu_{2-x}Se$ thin films from a thiocyanate bath using combined cyclic voltammetry and microgravimetry studies. The deposition of the $Cu_{2-x}Se$ thin film took place on a previously formed Se layer on the working electrode. The mechanism of the deposition

* Corresponding author. Fax: +56-32-273422. E-mail: rcordova@ucv.cl.

10.1021/jp047485o CCC: $30.25
Published on Web 01/27/2005

changed to a co-deposition of Cu and Se and a *M*/*z* ratio value was obtained, which was independent of the applied potential in the potential range, where the compound was formed. On the other hand, the deposition of $Cu_{2-x}Se$ at other potential values yielded different *M*/*z* values. This behavior was attributed to the different morphologies of $Cu_{2-x}Se$ films, which were deposited at different potential values. The same authors used thiocyanate as a complexing agent of Cu(I) to study the one-step deposition of $Cu_{2-x}Se$ and CIS.[12] The physical characterization using energy-dispersive X-ray spectrometry (EDXS), scanning electron microscopy (SEM), and XRD showed a good control of the stoichiometry achieved over a wide potential range, indicating that the film composition was controlled by an induced co-deposition mechanism. The electrochemical characterization of the CIS electroformation was also performed with an EQCM, and the results confirmed that CIS formation also proceeds via an induced co-deposition mechanism that involves the previous electroformation of the $Cu_{2-x}Se$ compound.[13] Under the experimental conditions reported in this work, the direct participation of binary In_ySe compounds was rejected.

In this work, Cu−Se phases were synthesized by the electrooxidation of copper in an alkaline medium containing selenide. In turn, stable selenide solutions were obtained by the redox dissolution of elemental selenium in a highly alkaline medium containing dithionite through a process represented by the following reaction

$$S_2O_4^{2-} + 4OH^- + Se \leftrightarrow 2\,SO_3^{2-} + 2\,H_2O + Se^{2-} \qquad \Delta G = -61.1\ \text{kJ}^{14} \quad (1)$$

To our knowledge, this procedure establishes a new route given that, in all the previous reports related to the electrosynthesis of Cu−Se compounds, they were founded on cathodic procedures mostly performed in acid electrolytic media.

From previous studies related to the electrochemical behavior of dithionite, in alkaline solutions on gold and platinum electrodes,[15,16] it is possible to predict that, under the experimental conditions proposed in current work, the electrooxidation of dithionite (that leads to sulfite in the first stage and then to sulfate ions as products) takes place in a potential range where there is no interference with the Cu−Se film electroformation.

A voltammetric study was performed in order to propose a mechanism for the electroformation of Cu−Se film. This mechanism was also supported by the results obtained from an EQCM study that was carried out in order to relate the variation of charge with mass variation during the process of the electroformation of a thin phase of Cu−Se compound. A *I*/*t* transient study was performed with the aim to gain insight on the nucleation and growth mechanisms of the Cu−Se phase electroformed under the experimental conditions assayed. Besides, a morphological study of the Cu−Se phase, electroobtained on a gold/crystal quartz-working electrode system, was conducted by means of atomic force microscopy (AFM). Finally, an EDXS assay on a film of Cu−Se compounds, obtained on a bulk copper electrode in a strongly alkaline medium, was carried out to determine the respective copper/selenium atomic ratio.

2. Experimental Section

Electrochemical experiments were performed in a single-compartment, three-electrode glass cell. The counter electrode was a large area platinum wire (5 cm^2), and the reference electrode was a saturated calomel electrode (SCE, 0.242 V vs NHE). All the potentials mentioned in the text refer to this electrode. Two types of working electrodes were used in this work: a bulk copper electrode with a geometrical area of 0.20 cm^2 and a thin film of copper electrodeposited on a Si/Au electrode system with a geometric area of 0.20 cm^2 (ELCHEMA). The quartz resonator was an AT-cut quartz crystal resonating at a fundamental frequency of 10 MHz. Before electrodepositing the copper film, the Si/Au electrode system was cleaned with a freshly prepared mixture of H_2SO_4/HNO_3 (1:1) for 2 min, followed by a copious rinse with Milli-Q water. Copper deposition took place when applying a potential step of −0.100 V by 40 s in a 50 mM $CuSO_4$, 10 mM Na_2SO_4 (pH 2.0) electrolytic solution. The mass of the copper deposit was ∼5000 ng. Then, the electrode was mounted on the electrochemical cell, exposing the copper surface to the electrolytic solution (0.05 M $Na_2B_4O_7$). Subsequently, by applying a potentiostatic pulse at a potential value of −1.5 V for 10 min, all copper species containing oxygen present on the electrode surface were reduced. Thus, an electrode system formed by a quartz/Au/Cu interface was obtained. On the other hand, the bulk copper electrode was polished with alumina (0.02 μm). The cyclic voltammetry technique was employed to characterize both types of copper electrodes in the potential range comprised between − 1.2 and 0.0 V, at a scan rate of 0.02 V s^{-1}.

The selenide ion solution was prepared in an ultrasonic bath under argon atmosphere, by the dissolution of elemental selenium (10 mM) in a 1 M NaOH, 60 mM $Na_2S_2O_4$ solution. Aliquots of this solution, freshly prepared, were added to the electrolyte (borate or 1 M NaOH solutions) in order to reach different final concentrations of selenide. The aliquots were added under polarization of the working electrode at −1.5 V, maintaining an inert atmosphere. The final pH of the borate electrolytic solutions was close to 10.

A voltammetric study was conducted with the electrodes in an electrolytic solution containing either 50 mM $Na_2B_4O_7$ or 1 M NaOH and 1 mM selenide, at a scan rate of 0.2 V $s^{-1} \geq \upsilon \geq 0.005$ V s^{-1}. At the beginning, a polarization step at −1.5 V for a period of 10 min was applied, followed by the addition of an aliquot of a standard selenide solution, maintaining the polarization for 10 additional minutes. The final concentration of selenide was 1 mM. A cyclic voltammetry program was applied, starting from the −1.5 V potential value. The potential range was from −1.5 to −0.6 V both in the positive going potential scan (PGPS) and in the negative going potential scan (NGPS). Nevertheless, when the purpose was to study the behavior of the electrode system covered by the Cu−Se phase initially formed, the anodic potential limit was extended to −0.2 V. The study of the potentiostatic *I*/*t* current transients with the bulk Cu electrode was performed in a 0.05 M $Na_2B_4O_7$, 5 mM HSe^- electrolytic solution. The applied *E*/*t* program considered an initial potential step at −1.5 V for 10 min; during the polarization, an aliquot of selenide solution was added to the electrolytic solution. Potential steps were applied in the potential range between −1.20 and −0.90 V. All the electrochemical experiments were carried out with a Zanher IM6e potentiostat/galvanostat. For the data acquisition and data analysis, a THALES package from Zahner Elektrik GmbH & Co was used. Nanoelectrogravimetric experiments were done with a PINE potentiostat (Pine Instrument Company, model RDE4) connected to an electrochemical quartz crystal microbalance (ELCHEMA, EQCN-501). All the experiments were performed at ambient temperature (18−20 °C) under argon atmosphere. Analytical grade reagents were employed. Morphology studies of the working electrode surface were performed ex situ with a Nanoscope IIIa instrument (Digital Instruments, Santa Barbara,

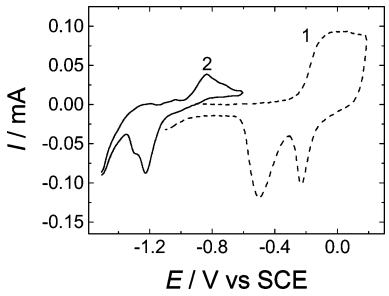

Figure 1. Cyclic voltammograms of Cu electrodes in 0.05 M $Na_2B_4O_7$ (pH 9.2). Scan rate 0.02 V s^{-1}: (1) in the absence of selenide ion; (2) in the presence of 1 mM selenide ion.

CA) using the tapping mode. The EDXS study of the Cu−Se film was performed with a JEOL 5410 scanning electron microscope with an EDXS microprobe. The film was obtained by the polarization of a bulk copper electrode for 2 h in a 1 M NaOH, 5 mM Se^{2-} electrolytic solution. The Cu−Se film formed was detached from the electrode surface using an adhesive tape and maintained under inert atmosphere and dry conditions previous to the analysis. All deconvoluted *I*/*E* and *I*/*t* profiles shown in this work, were achieved by applying a nonlinear curve-fitting program (Microcal Origin 5.0) reducing chi-square until a minimal and constant value was achieved. For the deconvolution processes of the *I*/*E* profiles, Gaussian peaks were considered and the number of them was in accordance with the electrochemical process that can be taking place in the respective potential range. For the *I*/*t* profiles, the respective equations used for the deconvolution process are showed in the corresponding section.

The contact angle measurements, of an argon bubble on the electrode surface as a function of the potential applied in the corresponding electrolyte, were performed with a RNL Rame Hart goniometer.

3. Results and Discussion

3.1. Voltammetry. Figure 1 shows the voltammetric *I*/*E* profiles of a quartz/Au/Cu working electrode system in a 50 mM $Na_2B_4O_7$ electrolytic solution. The voltammograms were recorded in the absence (dashed profile 1) and in the presence (profile 2) of selenide. Profile 1 shows a wide anodic current peak obtained in the PGPS that corresponds to the formation of copper oxides. The NGPS shows two cathodic current peaks that are related to the electroreductions of copper oxide species. The copper oxide species formation starts at −0.5 V versus SCE. In the NGPS, at a potential more negative than −0.7 V, the water discharge reaction takes place. The anodic and cathodic processes described above agree with previous results reported for the behavior of copper electrodes in alkaline media.[17−19] In the presence of selenide (profile 2), the PGPS shows a complex anodic current peak associated with the electroformation of a Cu−Se film. An anodic current prepeak located at −1.04 V precedes the principal current peak. Similarly, this current prepeak, which was described for the Cu/sulfide system,[19] would be attributed to the under-potential deposition (UPD) of a hydroselenide layer on the copper surface. In the NGPS, two coupled cathodic currents peaks located at −1.23 and −1.30 V, respectively, are clearly appreciated. These currents peaks are overimposed on an exponential current contribution that is due to the water discharge process (WDP).

As shown in Figure 1, the processes that involved the electroformation and electroreduction of the Cu−Se phases are located at potential values which are more negative than the respective processes corresponding to the copper oxides, according to the minor solubility of the Cu−Se compounds compared with the Cu−O compounds.

I/*E* profile 2 shows that the ΔE_p magnitude between the peak potential values of the main anodic and cathodic processes clearly indicates the irreversible character of the electrochemical processes.

The Q_a/Q_c charge ratio obtained from profile 2 was always lower than 1, showing that during the NGPS both take place: reduction of the copper selenide compounds electrochemically formed in the PGPS and WDP. Nevertheless, when the cathodic *I*/*E* profiles were deconvoluted (see below) in order to obtain the net electrical charge of the electroreduction of Cu−Se compounds, this Q_a/Q_c ratio was close to 1.

The linear relationship of the main anodic current peak (E_{pa}) with the scan rate (υ) is shown in Figure 2. The slope is close to $1.15RT/\alpha F$ ($\alpha = 0.5$) per decade of υ, meaning that the first electron transfer controls the electroformation of a Cu−Se phase. The effect of the scanning rate on the main anodic current peak value is shown in Figure 2B. The linear relationship between the current maximum (I_p) and $\upsilon^{1/2}$ reveals the existence of a totally irreversible diffusion controlled process.[20] According to the above potentiodynamic parameters, the following sequence of reactions can be proposed for the electroformation of a Cu−Se phase:

SCHEME 1: Mechanism Sequence for Electroformation of a Cu_xSe Phase, Where $2 \geq x/y \geq 1$

$$x\mathrm{Cu(H_2O)}_m + y\mathrm{HSe}^- \leftrightarrow \mathrm{Cu}_x(\mathrm{HSe})^-_{y_{ads}} + m\mathrm{H_2O} \quad (2)$$

$$\mathrm{Cu}_x(\mathrm{HSe})^-_{y_{ads}} \xrightarrow{\text{rds}} \mathrm{Cu}_x(\mathrm{HSe})^{(y-1)-}_y + \mathrm{e}^- \quad (3)$$

$$\mathrm{Cu}_x(\mathrm{HSe})^{(y-1)-}_y + y\mathrm{OH}^- \leftrightarrow \mathrm{Cu}_x\mathrm{Se}_y + y\mathrm{H_2O} + (2-y)\mathrm{e}^- \quad (4)$$

Similar results were obtained when the study of the Cu−Se electroformation was performed in 1 M NaOH (pH 14). In fact, the potentiodynamic parameters, $\partial \log I_p/\partial \log \upsilon$ and $\partial \Delta E_p/\partial \log \upsilon$ in the corresponding principal anodic current peak were 0.5 and 0.060 V dec^{-1}, respectively, indicating that the electroformation mechanism presents the same steps as those in eq 2−4, except for the fact that selenium species participate under the form of the selenide ion (Se^{2-}).

3.2. Nanoelectrogravimetric Study. Figure 3 shows the simultaneously recorded *I*/*E* and *m*/*E* cyclic potentiodynamic profiles covering the potential range from −1.50 to −0.6 V. The anodic and cathodic charges corresponding to the electroformation and electroreduction of Cu−Se phase were both 0.603 mC. This charge value was obtained after the deconvolution of the cathodic *I*/*E* profile (see below). From the beginning of the PGPS, mass increases monotonically until reaching a value close to 180 ng at the end of the anodic potential scan. This process is related to the growth of the different copper selenide compounds. As copper is present in the electrode, most of the net mass increase corresponds to the incorporation of selenium in the film.

In the NGPS registered from −0.60 to −0.98 V, mass increases until reaching a mass value close to 300 ng. This increase is related to the oxidation process that was initiated in the PGPS and corresponds to the growth of the different copper selenide compounds mentioned above. In the potential range from −0.90 to −1.5 V in the NGPS, mass begins to decrease concomitantly with the electroreduction of the Cu−Se phase formed. The final mass value attained was higher than the initial

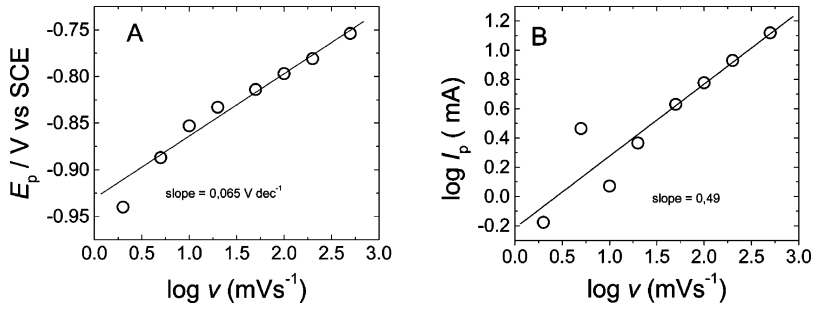

Figure 2. Potentiodynamic parameters related to the Cu_xSe formation: (A) variation of the potential current peak with the logarithm of scanning rate; (B) log variation of the anodic current peak with the scanning rate.

TABLE 1: Electrochemical Process and Electrical Charges Associated with the Current Peak Contributions Obtained from Figure 4

current contributions					
anodic	cathodic	electrochemical process		Q_a (mC)	Q_c (mC)
a1	c1	$xCu + HSe^- \leftrightarrow Cu_xHSe + e^-$	(5)	0.030	0.030
a2	c2	$(2-x)Cu + HSe^- + OH^- \leftrightarrow Cu_{2-x}Se + H_2O + 2e^-$	(6)	0.115	0.115
a3	c3	$3Cu + 2HSe^- + 2OH^- \leftrightarrow Cu_3Se_2 + 2H_2O + 4e^-$	(7)	0.310	0.310
a4	c4	$Cu + HSe^- + OH^- \leftrightarrow CuSe + H_2O + 2e^-$	(8)	0.148[a]	0.148
	c5	$2H_2O + 2e^- \rightarrow H_2 + 2OH^-$	(9)		

[a] Taking into account a charge of 0.126 mC in the NGPS not considered in the fitting treatment.

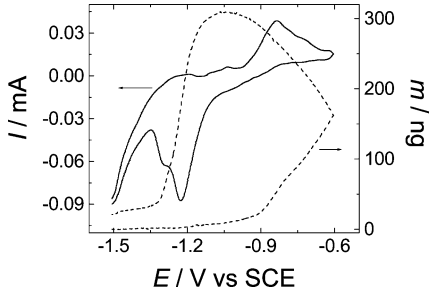

Figure 3. *I*/*E* (solid line) and *m*/*E* (dashed line) potentiodynamic profiles for a Au/Cu electrode in 0.05 M $Na_2B_4O_7$ (pH 9.2), 1 mM HSe^-. Scan rate 0.02 V s^{-1}.

mass value (∼20 ng). We attributed this fact to the different interfacial compositions that are present at both potentials; moreover, some selenide ions could be retained on the electrode after the complete electroreduction of the Cu−Se phase.

Due to the complex character of the anodic and cathodic *I*/*E* profiles, a deconvolution treatment was applied to both profiles in order to get a better definition of its respective current contributions. The deconvoluted *I*/*E* profiles were achieved by applying a nonlinear curve-fitting program. Gaussian shapes for the peaks were considered. The number of the Gaussian peaks assumed for the fitting procedure was accordance with the number of electrochemical processes that can be taking place in the respective potential range. Thus, in the PGPS and the NGPS, four and five peaks were considered, respectively, because a similar number of electrochemical processes can be occurring in the respective potential range.

The result of this treatment is displayed in Figure 4. Figure 4A shows three anodic current peak contributions located at −1.04 V (a1), −0.86 V (a2), and −0.76 V (a3), respectively, and a partial anodic current contribution (a4) that continues developing in the NGPS. On the other hand, Figure 4B shows four cathodic current peak contributions located at −1.02 V (c1), −1.14 V (c2), −1.22 V (c3), and −1.30 V (c4), respectively, and an exponential cathodic current contribution (c5) assigned to the WDP. This last contribution is present in the whole potential range where the cathodic *I*/*E* profile was registered.

The processes a1 and c1 correspond to the UPD of the hydroselenide layer,[19] and the process c5 is attributed to the WDP. The assignment of the other electrochemical process to the respective current contributions shown in Table 1 took into consideration the criterion that the more oxidizing Cu−Se compounds require more energy, both for electroformation and electroreduction.

The processes associated with the above current contributions and their respective electrical charges are shown in Table 1.

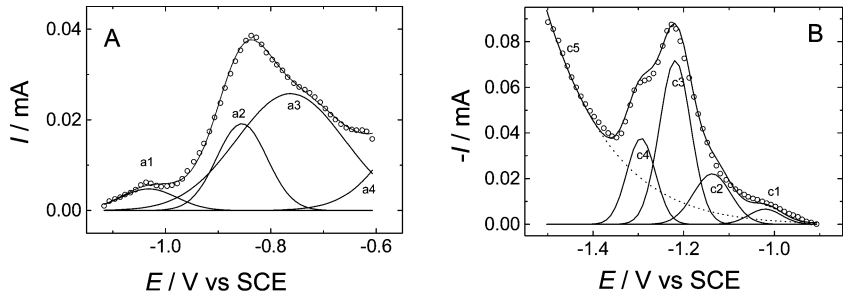

Figure 4. Deconvoluted *I*/*E* profiles for a Au/Cu electrode in 0.05 M $Na_2B_4O_7$ (pH 10), 1 mM HSe^-. Scan rate 0.02 V s^{-1}. Open circles represent the experimental *I*/*E* data, and solid lines represent the fitted *I*/*E* data: (A) anodic profile $Q_T = 0.603$ mC $= \sum_1^4 Q_a + Q_a^*$, $Q_a^* = 0.126$ mC in the NGPS and not considered in the fitting treatment; (B) cathodic profile, $Q_T = 0.603$ mC $= \sum_1^4 Q_c$.

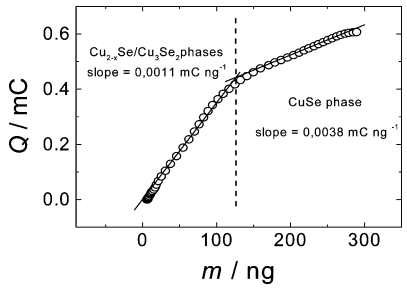

Figure 5. Plot of Q vs mass change obtained from Figure 3 for the anodic profile.

Therefore, the anodic and cathodic electrochemical processes follow the order $Cu_{2-x}Se$, Cu_3Se_2, and CuSe, where CuSe and $Cu_{2-x}Se$ represent the most and the least oxidized phases, respectively. In consequence, if it is considered that the Cu−Se compounds are arranged in successive layers following the above order and the respective direction of the electron flux, the CuSe compound would be located in the external area of the film, facing the electrolyte, and the $Cu_{2-x}Se$ compound would be located in the internal area of the film, facing the copper surface.

As shown in Figure 4A, the current contributions involved in the principal anodic current peak are a2 and a3, and they correspond to the processes represented by reactions 6 and 7. Therefore, the mechanism sequence showed in Scheme 1 (vide infra) is referred to the electroformation of $Cu_{2-x}Se$ and Cu_3Se_2 compounds.

When the anodic limit of the PGPS was fixed at −0.8 V (not shown), the respective deconvolution of the anodic and cathodic I/E profiles did not show the current contributions attributed to reaction 8 in Table 1. This fact indicates that the CuSe compound was not formed in this potential range.

Figure 5 shows a plot of electrical charge (Q) versus the mass variation (m) that takes place during the PGPS, which was obtained from the respective anodic I/E and m/E profiles of Figure 4. Two linear relationships with slopes of 3.8×10^{-3} and 1.1×10^{-3} mC ng^{-1} are observed, respectively. Considering that all the reactions shown in Table 1 involve two electrons for each selenium atom entering the film, from eq 10

$$M = n\frac{\Delta m}{\Delta Q_a}F \quad \text{with} \quad n = 2 \tag{10}$$

where F is the Faraday constant, molar mass values (M) of 51 and 175.4 g equiv^{-1} were obtained. The M value calculated from the first slope is lower than the mass value expected from the incorporation of one Se atom (78.96 g equiv^{-1}) into the Cu−Se film. This fact can be explained when we consider that each Se atom incorporated rejects 1.5 water molecules from the electrode surface. This exchange process takes place in the potential range where $Cu_{2-x}Se$ and Cu_3Se_2 are formed (−1.1 to −0.7 V). On the other hand, from the second slope, the M value calculated was 2.2 times greater than the mass value of one Se atom. In this case, the difference observed indicates that, in this potential range (−0.7 to −0.6 V), for each selenium atom incorporated to the CuSe phase, 1.2 selenide anions were specifically adsorbed. This fact is in accordance with the precipitation theory that establishes that an insoluble phase always tends to adsorb those common ions, which are in excess in the medium where the insoluble phase is formed.[21]

The departure of the water molecules from the electrode surface does not change the hydrophilic characteristic of the surface. In fact, when the contact angle between the electrode surface and an Ar bubble was measured at −1.2 V versus SCE in the electrolyte containing selenide anion (where the copper surface remain unharmed), the angle was 0°. The same value was obtained at −0.8 V versus SCE, where the Cu/Se phases were formed.

When the same experiment was done in 1 M NaOH with an anodic potential limit of −0.8 V (not shown), two slopes for the relationships Q versus m were also obtained. The respective slope values were 2.9×10^{-3} and 0.9×10^{-3} mC ng^{-1}. In this case, the M values obtained from each slope value were 66.5 and 214.4 g equiv^{-1}, respectively. Therefore, considering the same arguments, 0.7 H_2O molecules are rejected from the electrode surface (first slope value) and 1.7 selenide anions are adsorbed (second slope value) for each selenium atom incorporated to the Cu−Se phase, respectively.

On the basis of the above, it is possible to conclude that, during the electroformation of the $Cu_{2-x}Se$ and Cu_3Se_2 phases, the electrode exchanges previously absorbed water molecules for each selenium atom incorporated to the film. This process ended when the whole electrode surface was covered by these phases. In the following oxidation processes, besides the incorporation of more selenium atoms for attaining the formation of the CuSe compound, specific adsorption of selenide anions takes place.

Consequently, the global process that would lead to the electroformation of Cu−Se phases, with different stoichiometry, can be expressed as follows:

Preliminary State

$$Cu_x[nH_2O]_{ads} + ySe^{2-} \rightarrow Cu_xSe_y + nH_2O + 2ye^- \tag{11}$$

where $x/y < 2$ and $2 > n \geq 0.7$

Subsequent State

$$Cu/Cu_xSe_y + (1+z)Se^{2-} \rightarrow Cu_xSe_y/CuSe[zSe^{2-}] + 2e^- \tag{12}$$

where $1 \leq z < 2$

Therefore, the Cu−Se phases involved in the processes described above are $Cu_{2-x}Se$ and Cu_3Se_2 for the preliminary stage and CuSe for the subsequent ones. The stoichiometry Cu_2Se phase is not considered in the present discussion because such a compound is not thermodynamically stable under the experimental conditions assayed.[22]

In turn, when the total cathodic charge ($Q_c = 0.603$ mC) and the respective mass variation ($\Delta m = 282.5$ ng) are considered, the resulting $\Delta Q_c/\Delta m$ ratio is 2.1×10^{-3} mC ng^{-1}. From this figure and applying eq 12, an M value of 91.89 g is determined. This M value is slightly greater than the atomic mass of selenium (78.96 g mol^{-1}), which is leaving the electrode due to electroreduction of the Cu−Se compounds. This means that selenium anions, specifically adsorbed in the PGPS, are partially desorbed during the electroreduction process. This fact could explain why the final mass attained is greater than the initial one after the electroreduction of Cu−Se compounds is finished.

Figure 6 shows the simultaneous I/E and m/E cyclic potentiodynamic profiles covering the potential range from −1.50 to −0.2 V. In this figure, three anodic current peaks (a1, a2, and a3) in the PGPS and two cathodic current peaks (c1 and c2) in the NGPS are observed. The current peaks assigned as a1 and c2 are related to the electroformation and electroreduction of Cu−Se phases, respectively. The current peak a2, which starts at a potential value close to −0.8 V, could correspond to the oxidation of metallic copper (underlying the $Cu_{2-x}Se$ and Cu_3-

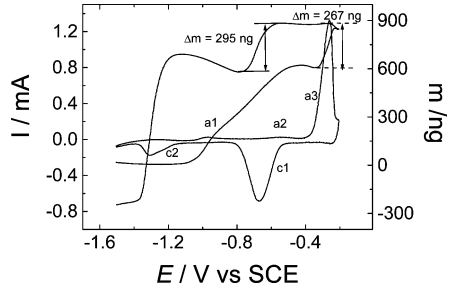

Figure 6. *I*/*E* (solid line) and *m*/*E* (dashed line) potentiodynamic profiles for Au/Cu in 0.05 M $Na_2B_4O_7$ (pH 9.2), 1 mM Se^{2-}. Scan rate 0.02 V s^{-1}.

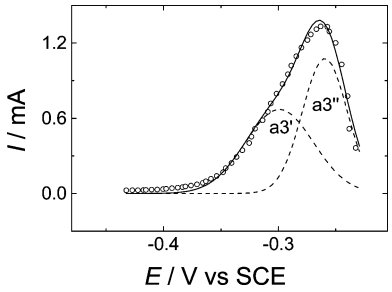

Figure 7. Deconvoluted anodic *I*/*E* profile corresponding to peak 3 of Figure 6: experimental *I*/*E* data (open circles); fitted *I*/*E* data (solid line); electroformation of Cu_2O (a3′); electroformation of CuO (a3″).

Se_2 phases) to a Cu(II) selenide phase according to the following reaction

$$Cu/Cu_{2-x}Se/Cu_3Se_2x[Se^{2-}]_{ads} + Se^{2-} \rightarrow Cu_{2-x}Se/Cu_3Se_2/CuSex[Se^{2-}]_{ads} + 2e^- \quad (13)$$

In this reaction, $[Se^{2-}]_{ads}$ represents selenide anions adsorbed on the Cu−Se phases. On the other hand, the anodic current peak 3 would correspond to the electrooxidation of underlying copper to copper(I) oxide and, then, from copper(I) to copper(II) oxide, through the Cu−Se phases previously formed. This process occurs with a partial desorption of selenide anions, as follows:

$$Cu/(Cu-Se\ phases)x[Se^{2-}]_{ads} + 2OH^- \rightarrow (Cu-Se\ phases)(x-z)[Se^{2-}]_{ads}/CuO + H_2O + zSe^{2-} + 2e^- \quad (14)$$

The term Cu−Se phases, considered in eq 14, corresponds to the mixture of $Cu_{2-x}Se$, Cu_3Se_2, and CuSe compounds remaining on the electrode. When the anodic *I*/*E* profile corresponding to the current peak a3 is deconvoluted in the potential range −0.4 to −0.2 V, two anodic contributions are displayed (Figure 7). The corresponding current peak potentials are located at −0.30 V (a3′, Q_a = 2.48 mC) and −0.26 V (a3″, Q_a = 2.48 mC), and they would be assigned to the electroformation, first of Cu_2O from copper, followed by the oxidation to Cu_2O previously formed to CuO.

It is remarkable that the current peaks a3 and c1 were not dependent on the hydrodynamic condition of the solution and that their total charge ratio (Q_a/Q_c) was close to 1. Therefore, in the NGPS (cathodic current peak c1 in Figure 6), copper(II) oxide is reduced in one single process to another insoluble phase, which also remains on the electrode surface. For this process, the following reaction is proposed:

$$(Cu-Se\ phases)(x-z)[Se^{2-}]_{ads}/CuO + ySe^{2-} + H_2O + 2e^- \rightarrow (Cu-Se\ phases)(x-z+y)[Se^{2-}]_{ads}/Cu + 2OH^- \quad (15)$$

To support the processes represented by eqs 14 and 15, the variation of electrical charge with mass was considered. Figure 8A shows a plot of anodic charge (Q_a) versus mass variation (*m*). The data were obtained from Figure 6 in the potential range from −0.45 to −0.2 V. where the anodic current peak a3 is developed. Only a linear relationship with a slope ($\Delta Q/\Delta m$) of 1.9×10^{-2} mC ng^{-1} was obtained. From this slope value and using eq 10, a molar mass value of 10.16 g mol^{-1} was calculated. This mass value is lower than the theoretical mass value (16 g mol^{-1}) expected from reaction 14 (incorporation of one oxygen atom for a two-electron process). This difference is attributed to the fact that, together with the electrooxidation of Cu to CuO, selenide anions previously adsorbed on the Cu−Se phases are partially released from the electrode surface. The amount of selenide anion desorbed (*z*) can be estimated as 0.07 selenide anions by each oxygen atom incorporated as CuO. As can be seen in Figure 6, an initial decrease in mass is observed in the *m*/*E* profile when anodic peak 3 starts, supporting desorption of selenide anion from the electrode.

Similarly, Figure 8B displays the variation of the cathodic charge (Q_c) with mass variation (*m*). The data were obtained from Figure 6 in the potential range from −0.40 to −0.8 V in the NGPS. In this case, two linear relationships with slopes ($\Delta Q/\Delta m$) of -2.3×10^{-2} and -1.2×10^{-2} mC ng^{-1} were obtained, respectively. From the first slope value, a molar mass of 8.4 g mol^{-1} was obtained, which is lower than the theoretical mass value (16 g mol^{-1}) expected from reaction 15 due to the release of one oxygen atom for every two electrons in the process. This is due to the fact that, together with the release of oxygen atoms, selenide anions (0.1 mol) are incorporated to the electrode. From the second slope, a molar mass of 16.1 g mol^{-1} was calculated, which is close to the expected molar mass.

On the other hand, the total charge corresponding to the electroreduction of all Cu−Se compounds involved in cathodic peak 5 (Q_c = 0.87 mC) is close to the sum of the electrical charges of the anodic current peaks 1 and 2 (0.82 mC). As

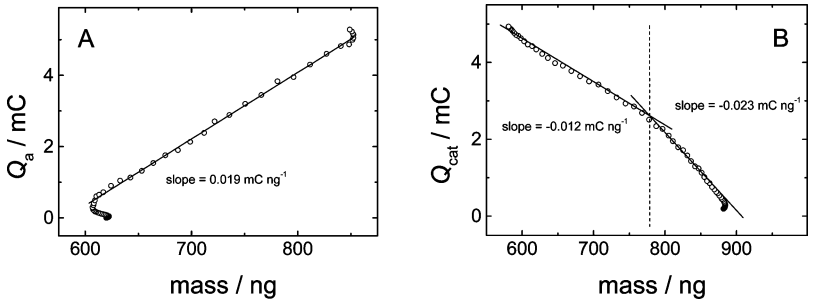

Figure 8. Plot of *Q* vs mass change obtained from Figure 6 (A) for anodic current peak 3 and (B) for cathodic current peak 4.

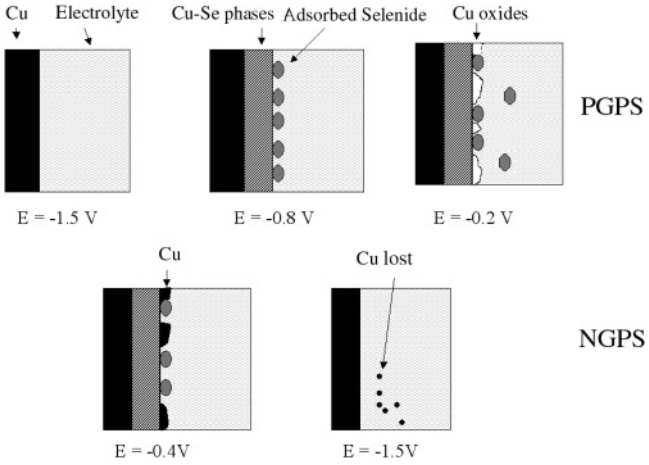

Figure 9. Schematic representation for the different stages occurring in the electroformation and electroreduction of the Cu−Se compound processes in 0.05 M $Na_2B_4O_7$, 5 mM HSe^- electrolytic solution.

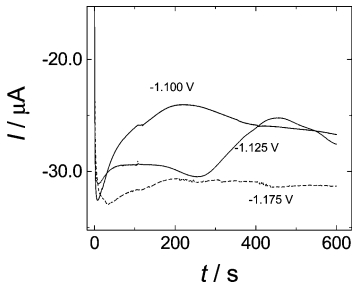

Figure 10. *I*−*t* transients obtained with a bulk copper electrode in 0.05 M $Na_2B_4O_7$, 5 mM HSe^- electrolytic solution at the potentials assigned.

shown in the *m*/*E* profile in Figure 6, the final mass value attained (−243 ng) is lower than the initial mass value. The difference could be attributed to a partial loss of elemental copper from the electrode as a result of the release of selenide anions during the electroreduction of Cu−Se phases.

A schematic representation of the processes related to the electroformation and electroreduction of Cu−Se phases is shown in Figure 9.

Is necessary to mention that, in the above discussion, where *Q*/*m* relationships were considered, the effect of the roughness electrode variation on the mass and charge measurements was not considered. This assumption was founded in the fact that the root mean square (rms) values obtained from the AFM images of the electrode surfaces Si/Au/Cu and Si/Au/Cu_xSe do not change more than a percentage value close to +12%.

3.3. Potential Step Experiments. Figure 10 displays various experimental *I*−*t* transients for the electrodeposition of Cu−Se phases on a bulk copper electrode. They were obtained by holding the initial potential of a copper electrode at −1.50 V for 10 min and then stepping to a final applied potential (E_s) ranging from −1.20 to −1.10 V in a 0.05 M $Na_2B_4O_7$ (pH 9.2), 5 mM Se^{2-} electrolytic solution. A remarkable fact is that, in all the cases, the current values measured were always negative because of the participation of the WDP. Therefore, the instantaneous current values measured were the result of the cathodic current due to this process (major process) and of the anodic current corresponding to the electroformation of the Cu−Se phase (minor process). Despite the presence of the WDP, the *I*−*t* transients showed the typical shape of a nucleation process. At a very early stage (t < 1 s), the double-layer charging occurs and then the current increases due to the formation and growth of the nuclei. The instantaneous current rises until it reaches a maximum value and finally tends to decrease.

All the experimental *I*−*t* transients show various current maximums, revealing that the nucleation and growth mechanism (NGM) of a Cu−Se phase is a complex process that takes place over different stages.

To analyze the *I*−*t* transients, the corresponding nondimensional parameters I/I_m and t/t_m were obtained and compared with the respective parameters for the theoretical NGM: instantaneous bidimensional (IN2D) or progressive bidimensional (PN2D). As an example, Figure 11 shows different nondimensional plots for the *I*−*t* transient obtained at a potential value of −1.125 V. In Figure 11A, a good fit with the theoretical plot corresponding to a NI2D mechanism is observed at short times. At longer times (Figure 11B), the nondimensional plot fits adequately with the theoretical plot corresponding to a NP2D mechanism.

Also, the *I*−*t* transient obtained at times longer than 250 s, at a potential value of −1.125 V, shows at least three current maximums (Figure 10). When this *I*−*t* transient was analyzed using nondimensional plots, in the lapse of time where the respective maximum appears, a good fit with a NP2D mechanism is appreciated (Figure 12). Similar results (not shown) were obtained for the other *I*−*t* transients analyzed. Summarizing, the complete nucleation mechanism that describes the electroformation of a Cu−Se phase appears to be composed by different processes: an initial IN2D mechanism followed by four PN2D mechanisms, with the last ones having different constant times. The IN2D process could be due to the selenization of superficial copper ions produced by oxidation, which leads to the production of a first irregular film of Cu−Se compounds. The PN2D processes are due to selenization of the copper ion, which goes though the preliminary film to the film/electrolytic solution interface where the corresponding chemical reaction occurs. Therefore, the PN2D processes are dependent on the thickness of the preliminary film that the copper ions must cross, which would explain the different times constant observed for each one of these PN2D processes. Consequently, the complex NGM should correspond to a layer-by-layer growth.

The next step was to fit the experimental *I*/*t* transient on the basis of the above considerations. To allow the corresponding fitting analysis, the negative current values of the *I*/*t* transients were converted to positive current values. For this purpose, the stationary current value measured at the initial potential step (−1.5 V) was considered as the zero current value. The deconvoluted *I*/*t* profiles were achieved by applying a nonlinear curve-fitting program. The shapes of the corresponding contributions are defined by the respective mathematical expression previously described in the literature.[23−26]

In addition to the NGM processes that take place, it was necessary to consider the current contribution which was due to the WDP. This process, as considered in previous studies,[23,24] follows the exponential law represented by eq 16:

$$I_{H_2} = a(1 - \exp(-bt^2)) \qquad (16)$$

In this equation, I_{H_2} is the current related to WDP, t is the time considered, and a and b are constants that depend of the potential value applied. Both constants were evaluated by a nonlinear fit procedure.

To carry out the fitting procedure in a simple way, the transients obtained at −1.125 V were simulated during the first 250 s. The instantaneous anodic current average is considered as the sum of different partial current contributions: the WDP

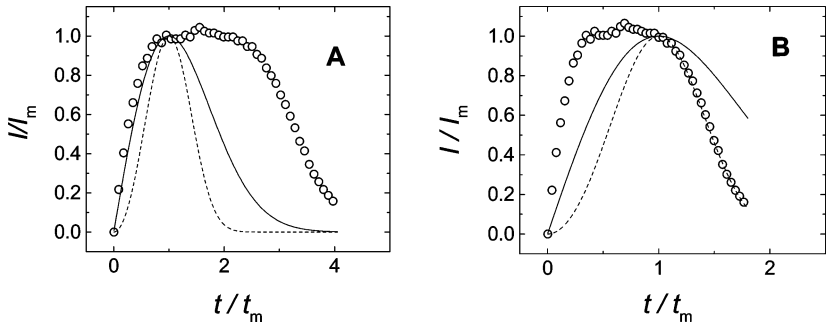

Figure 11. Nondimensional plot for the 2D nucleation of the Cu_xS phase on a bulk copper electrode obtained from the *I*/*t* transient at −1.125 V for (A) short times and (B) longer times: IN2D (solid line); PN2D (dashed line); experimental data (open circles).

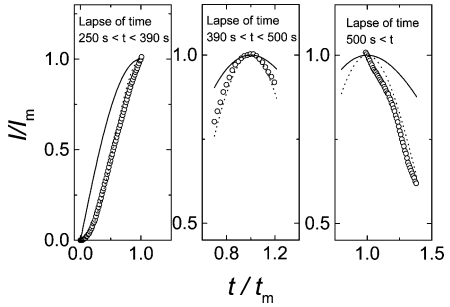

Figure 12. Nondimensional plot for the 2D nucleation of the Cu−Se phase on a bulk copper electrode obtained from the *I*/*t* transient at −1.125 V for times longer than 250 s (data obtained from Figure 9): IN2D (solid line); PN2D (dotted line); experimental data (open circles).

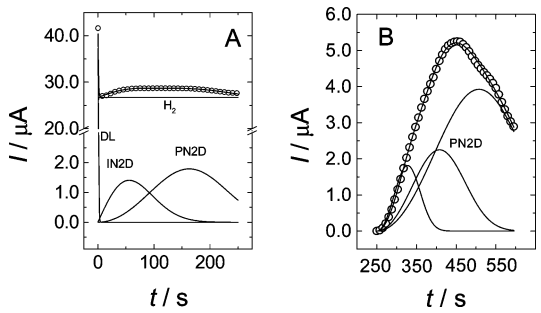

Figure 13. *I*/*t* transient obtained with a Au/Cu electrode in 0.05 M $Na_2B_4O_7$, 5 mM HSe^- at the potential −1.125 V. The open circles represent the experimental curve, and the lines represent the fitted curves (individual contributions I_{DL}, I_{H_2}, I_{IN2D}, and I_{PN2D}): (A) period of time of 0 to 250 s; (B) a period of time longer than 250 s.

(I_{H_2}), the double-layer charging (I_{DL}), and two contributions (I_{IN2D} and I_{PN2D}) due to the electroformation of the Cu−Se phase. The contribution I_{DL} is given by eq 17

$$I_{DL} = A \exp\left(-\frac{t}{B}\right) \tag{17}$$

where $A = \Delta V/R$ and $B = RC$. ΔV is the amplitude of the potential step, R is the resistance of the electrode/electrolyte interface, and C represents the capacity of the interface.[25]

I_{IN2D} represents the current transient contribution associated with a IN2D process under activated control [26] and follows eq 18

$$I_{IN2D} = Ht \exp(-Lt^2) \tag{18}$$

where $H = 2\Pi FMhN_0K\rho^{-1}$ and $L = \Pi N_0K^2M^2\rho^{-2}$. F is the Faraday constant, M is the molecular weight, N_0 and h are the number and height of the copper cluster, respectively, K is the rate of this nucleation process, and ρ is the density of the Cu−Se phase formed.

I_{PN2D} represents the current transient contribution associated with a PN2D process under activated control[26] and follows eq 19

$$I_{PN2D} = Ht^2 \exp(-Lt^3) \tag{19}$$

where $H = \Pi FMhAN_0K^2\rho^{-1}$ and $L = \Pi AN_0K^2M^2(3\rho)^{-2}$.

Figure 13A shows the *I*−*t* transients corresponding to a period of time shorter than 250 s. The respective partial contributions are also plotted. It is observed that the sum of all the contributions adequately fits the experimental *I*−*t* transients. At times longer than 250 s (Figure 13B), the stationary current value due to the WDP was not considered in the respective plot. For this reason, the instantaneous average anodic current of the *I*−*t* transient was fitted using an equation which considers only the three NP2D contributions. Once again, it is possible to observe a good fit between the experimental and the simulated data.

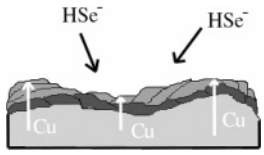

Figure 14. Model that represents the NGM of Cu−Se compounds on a Au/Cu electrode in 0.05 M $Na_2B_4O_7$, 5 mM HSe^-: Cu layer (light gray); Cu−Se layer by the IN2D mechanism (dark gray); Cu−Se layer by the PN2D mechanism (gray).

A model that represents the NGM of the Cu−Se phases formed is shown in Figure 14. The first layer is produced by a IN2D mechanism, and the subsequent ones are produced by means of NP2D mechanisms with different constant times because copper ion must cross an irregular existing film of different thickness.

3.4. AFM Study of the Cu−Se Film. To study the morphology of the Si/Au, Si/Au/Cu, and selenized Au/Cu film electrodes, the 3D AFM images of these electrodes were obtained, and they are shown in Figure 15. Figure 15a shows the morphology of the surface of a Si/Au electrode, where a flat surface and the wall of a neighboring terrace are separated by a furrow. Figure 15b shows the surface of a Au/Cu film electrode. This figure illustrates that the copper and/or copper-containing oxygen particles are widely spread in the entire electrode surface, covering terraces and furrows and modifying the topography of the Si/Au electrode. On the other hand, Figure 15c shows a selenized Si/Au/Cu electrode with a strong morphology change compared to the previous surfaces shown.

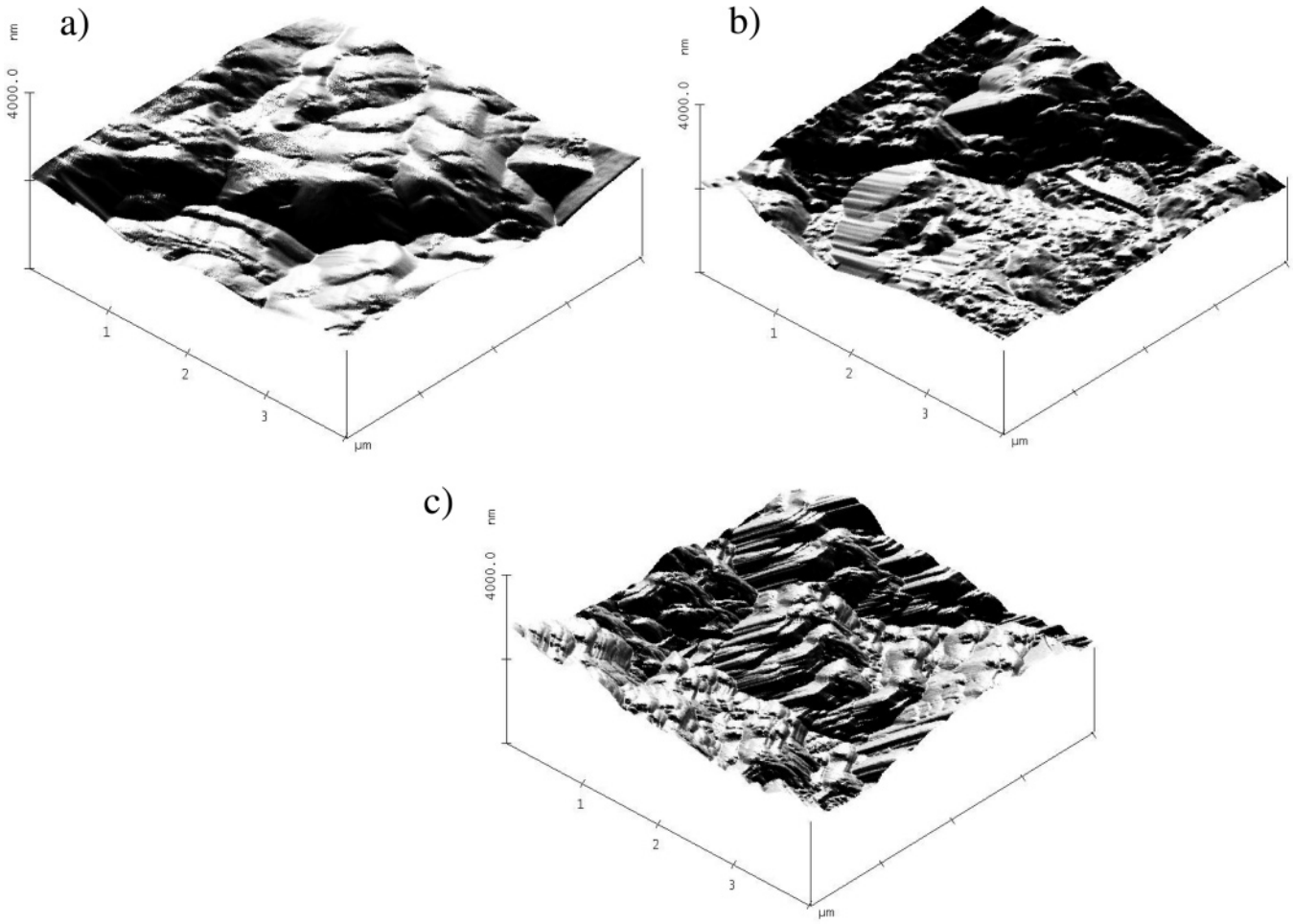

Figure 15. AFM images for (a) a Au surface electrode, (b) a Au/Cu surface electrode, and (c) a Au/Cu_xSe surface electrode.

TABLE 2: Electrical Charges Associated with Cathodic Current Contributions after the Application of an Anodic Potentiodynamic Scan in the Potential Range −1.5 to − 0.8 V for a Bulk Copper Electrode in a 1 M NaOH, 1 mM Se^{2-} Electrolytic Solution

compound electroreduced	$-E_p$ (V)	Q_c (mC)	%Q	Cu atomic fraction	Se atomic fraction
CuSe	1.28	0.058	13.2	0.132	0.132
Cu_3Se_2	1.25	0.187	42.6	1.278	0.852
$Cu_{2-x}Se^a$	1.20	0.194	44.2	0.884	0.442
total		0.439	100	2.294	1.426

[a] $x \rightarrow 0$.

The most important aspect of this image is the presence of a surface clearly structured in layers. This evidences the fact that the selenization process of a copper surface takes place by means of a layer-by-layer growth, as could be derived from the NGM study.

3.5. EDXS Study of the Cu−Se Film. The EDAX analysis of a Cu−Se film, prepared by polarization for 2 h at the potential −0.8 V of a bulk copper electrode in a 1 M NaOH, 5 mM Se^{2-} electrolytic solution, showed a Cu/Se atomic ratio of 1.60. The same atomic ratio was obtained from the charges associated with the corresponding cathodic current contributions after a potentiodynamic scan with an anodic limit potential of −0.8 V was applied to the same system (see Table 2). The data of Table 2 and the EDXS analysis showed that in this anodic potential interval the only Cu−Se phases present were $Cu_{2-x}Se$, Cu_3Se_2, and CuSe.

4. Conclusions

(1) Cyclic voltammetry (CV) parameters showed that the formation of $Cu_{2-x}Se$ and Cu_3Se_2 phases on a Au/Cu film electrode occurred through an irreversible diffusion controlled mechanism with a first electron transfer as the rate-determining step.

(2) CV and EQCM data support that the phases formed were $Cu_{2-x}Se$ and Cu_3Se_2 when the anodic potential limit was restricted to −0.8 V. When the anodic potential limit was extended to −0.6 V, a CuSe phase was also electroformed. When the anodic potential limit was extended to −0.2 V, copper oxide compounds were formed on the previous Cu−Se phases.

(3) Cathodic electrical charge analysis and EDXS analysis for the system Cu bulk/1 M NaOH, 1mM Se^{2-} revealed that, at a anodic potential limit of −0.6 V, a mixture of $Cu_{2-x}Se$, Cu_3Se_2, and CuSe compounds was formed.

(4) The I/t transient study showed that the NGM of Cu−Se phases corresponded to an initial IN2D mechanism followed by four PN2D mechanisms. Charge transfer controlled all the processes, and the film growth was a layer-by-layer mechanism.

(5) The AFM study showed that the deposit of Cu−Se phases appears as a layered film, supporting the mechanism obtained from the I/t transient study.

Acknowledgment. Dedicated to Professor D. Carrillo on the occasion of his 65th birthday. We gratefully acknowledge the financial support from FONDECYT-Chile (projects L.C. 8000022 and 3010016) and DGI-PUCV. M.O. thanks the Doctoral fellowship granted by MECESUP/UCO-9905.

References and Notes

(1) Mishra, K. K.; Rajeshwar, K. *J. Electroanal. Chem.* **1989**, *271*, 279.
(2) Molin, A. N.; Dikusar, A. I.; Kiosse, G. A.; Petrenko, P. A.; Sokolovsky, A. I.; Saltanovsky, Yu. G. *Thin Solid Films* **1994**, *237*, 66.
(3) Molin, A. N.; Dikusar, A. I. *Thin Solid Films* **1994**, *237*, 72.
(4) Thouin, L.; Massaccesi, S.; Sanchez, S.; Vedel, J. *J. Electroanal. Chem.* **1994**, *374*, 81.
(5) Bhattacharya, R. N.; Fernandez, A. M.; Contreras, M. A.; Keane, J.; Tennant, A. L.; Ramanathan, K.; Tuttle, J. R.; Noufi, R. N.; Hermann, A. M. *J. Electrochem. Soc.* **1996**, *143*, 854.
(6) Haram, S. K.; Santhanam, K. S. V. *J. Electroanal. Chem.* **1995**, *396*, 63.
(7) O'Brian, R. N.; Santhanam, K. S. V. *J. Electroanal. Chem.* **1989**, *260*, 231.
(8) Pejova, B.; Grozdanov, I. *J. Solid State Chem.* **2001**, *158*, 49.
(9) Marlot, A.; Vedel, J. *J. Electrochem. Soc.* **1999**, *146*, 177.
(10) Riveros, G.; Henríquez, R.; Córdova, R.; Schrebler, R.; Dalchiele, E. A.; Gómez, H. *J. Electroanal. Chem.* **2001**, *160*, 2001.
(11) Kemell, M.; Saloniemi, H.; Ritla, M.; Leskelä, M. *Electrochim. Acta* **2000**, *45*, 3737.
(12) Kemell, M.; Ritala, M.; Saloniemi, H.; Leskelä, M.; Sajavaara, T.; Rauhala, E. *J. Electrochem. Soc.* **2000**, *147*, 1080.
(13) Kemell, M.; Saloniemi, H.; Ritala, M.; Leskelä, M. *J. Electrochem. Soc.* **2001**, *148*, C110.
(14) Pourbaix, M. *Atlas of Electrochemical Equilibria in Aqueous Solutions*, 2nd ed.; National Association of Corrosion Engineers: Houston, TX, 1974 p 541, 546, 555.
(15) Westbroek, P.; De Stycker, J.; Van Uytfanghe, K.; Temmerman, E. *J. Electroanal. Chem.* **2001**, *516*, 83.
(16) Gasana, E.; Westbroek, P.; De Wael, K.; Temmenrman, E.; De clerck, K.; Kiekens, P. *J. Electroanal. Chem.* **2003**, *553*, 35.
(17) Collisi, U.; Strehblow, H.-H. *J. Electroanal. Chem.* **1990**, *284*, 385.
(18) Vásquez Moll, D.; DeChialvo, M. R. G.; Salvarezza, R. C.; Arvia, A. *Electrochim. Acta* **1985**, *30*, 1011.
(19) de Tacconi, N. R.; Rajeshwar, K.; Lezna, R. O. *J. Phys. Chem.* **1996**, *100*, 18234.
(20) Nicholson, R. S.; Shain, I. *Anal. Chem.* **1964**, *36*, 706.
(21) Erdey, L. *Gravimetric Analysis*; The Mcmillan Co: New York, 1963; Vol. 1, p 101.
(22) Ogorelec, Z.; Mestik, B.; Devčić, D. *J. Mater. Sci.* **1972**, *7*, 967.
(23) Córdova, R.; Gómez, H.; Schrebler, R.; Cury, P.; Orellana, M.; Grez, P.; Leinen, D.; Barros-Barrado, J. R.; del Río, R. *Langmuir* **2002**, *18*, 8647.
(24) Del Río, R.; Basaure, D.; Schrebler, R.; Gómez, H.; Córdova, R. *J. Phys. Chem B* **2002**, *106*, 12684.
(25) Beaunier, L.; Cachet, H.; Froment, M.; Maurin, G. *J. Electrochem. Soc.* **2000**, 147, 1835.
(26) Southampton Electrochemistry Group. *Instrumental Methods in Electrochemistry*; Ellis Horwood: Chichester, U.K., 1985; Chapter 3.